Digital Image Processing (DIP)

Project Report on

‘Automatic detection of microaneurysms in color fundus images’

By

Ritu Lahoti

Under the guidance of

Prof. Neelam Sinha

May, 2020

International Institute of Information Technology Bangalore (IIITB)

TABLE OF CONTENTS

Sr. No.	Topic	Pg. No.
	LIST OF FIGURES	**i**
1.	**INTRODUCTION**	
	1.1 Abstract	1.
	1.2 Objective of Project	1.
	1.3 Domain Knowledge	2.
2.	**REVIEW OF LITERATURE**	3.
3.	**IMAGES PROCESSING**	
	3.1 Database	4.
	3.2 Block Diagram	5.
	3.3 Pre-processing	
	3.3.1 Denoising and smoothing	5.
	3.3.2 Contrast Enhancement	6.
	3.3.3 Shade correction	6.
	3.4 MA Candidates detection	
	3.4.1 Top-hat filtering	7.
	3.4.2 Diameter closing	7.

Sr. No.	Topic	Pg. No.
4.	**FEATURE EXTRACTION AND CLASSIFICATION**	
	4.1 Feature Extraction from MA candidates	
	4.1.1 Shape based features	8.
	4.1.2 Intensity based features	8.
	4.2 Classification of detected MA candidates	
	4.2.1 Naive Bayes	10.
	4.3 Algorithm	
5.	**RESULTS AND DISCUSSION**	13.
6.	**CONCLUSION AND FUTURE SCOPE**	17.
	REFERENCES	18.

LIST OF FIGURES

Figure No.	Figure Caption	Pg. No.
Figure 1.2	Actual MA photography	1.
Figure 1.3	Fundus Images: Color, Red-, Green-, Blue-channel, FA	2.
Figure 3.1	Color fundus Images and their green channel	4.
Figure 3.2	Block diagram	5.
Figure 3.3.1	Denoising and Smoothing	5.
Figure 3.3.2	Contrast enhanced	6.
Figure 3.3.3	Shade Corrected	7.
Figure 3.4.2	Blood vessels extracted and MA Candidates detected	7.
Figure 3.5	Feature Vector Trained Dataset	9.
Figure 3.6	MA candidates classified as MA and non-MA	11.
Figure 5.1	Confusion matrix	13.
Figure 5.2	Output image 1	14.
Figure 5.3	Output image 2	15.
Figure 5.4	Output image 3	15.
Figure 5.5	Output image 4	16.

1. INTRODUCTION

1.1 ABSTRACT

The paper addresses the automatic detection of microaneurysms in color fundus images, which plays a key role in computer assisted diagnosis of diabetic retinopathy, a serious and frequent eye disease. [1] The algorithm can be divided into four steps. The first step consists in image enhancement, shade correction and image normalization of the green channel. The second step aims at detecting candidates, i.e. all patterns possibly corresponding to MA, which is achieved by diameter closing and an automatic threshold scheme. Then, features are extracted, which are used in the last step to automatically classify candidates into real MA and other objects; the classification relies on kernel density estimation with variable bandwidth. [1]

1.2 OBJECTIVE OF PROJECT

- Diabetic retinopathy (DR) is one of the most serious and most frequent eye diseases in the world; it is the most common cause of blindness in adults between 20 and 60 years of age.
- The main cause of the disease is the elevation of glucose in the blood, resulting in an alteration of the vascular walls whose first manifestations are microaneurysms (MA), tiny dilations of the capillaries.

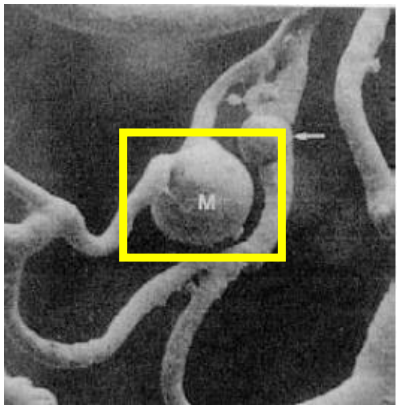

Figure 1.2 Actual MA photography [2]

- Microaneurysms itself does not affect vision, but progression of DR to later stages leads to complications such as new vessels and macular edema possibly leading to vision impairment and blindness.

- Such complications can be prevented by proper treatment if the disease is detected early enough, thereby preventing vision impairment and blindness.

- Automatic detection plays a key role for both;
    - *Mass-screening*: To identify automatically all ‘‘abnormal’’ retinas, i.e. all color images showing typical lesions/MA for DR
    - *Monitoring*: To trace the progression of disease for the efficiency assessment of a treatment or of a new drug.

1.3 DOMAIN KNOWLEDGE

- Microaneurysms are tiny dilations of the capillaries whose diameter ranges from 10µm to 100µm (<125µm). They are round in shape, and their color is similar to blood vessels (red) in color fundus image.
- Appearance of MA in fundus image (For this project, green channel is used);
  Color fundus images: They appear as small reddish isolated patterns of circular shape.
  Green channel of color images: They appear as dark, circular, small, isolated patterns.
  Fluorescein Angiographies (FA): They are bright circular patterns of better contrast.

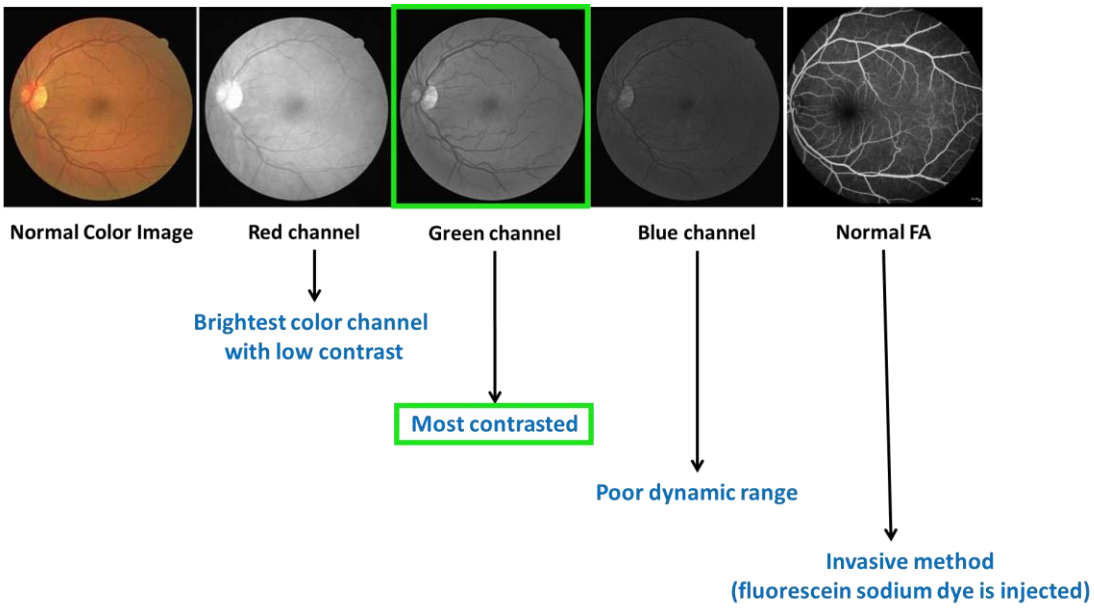

Figure 1.3 Fundus Images: Color, Red-, Green-, Blue-channel, FA

2. REVIEW OF LITERATURE

Different approaches along with image processing methods have been used to detect and identify microaneurysm candidates. Following technical papers have been referred for the same.

[1] Automatic Recognition of Microaneurysms in Diabetic Retinopathy by Lay et.al, 1983 (FA) [3]

The paper involves morphological openings with linear structuring elements in different directions. This removes MA but preserves the piecewise linear vessels. Such image is subtracted from original image (top-hat transformation) to extracts MA details.

[2] Automated detection and quantification of microaneurysms in fluorescein angiograms by Spencer, 1991 et al. (FA) [4]

The paper presents shade correction (remove unwanted changes in intensity). The microaneurysms were detected by means of a matched filter approach (Matched filters are of same size and shape as MA with a square matrix having values corresponding to the grey levels of the MA-prior knowledge).

[3] Automatic Detection of Microaneurysm in Retinal Fundus Images by Bo Wu, Weifang Zhu, Fei Shi, Shuxia Zhu, Xinjian Chen 2016 (Inverted Green Channel) [5]

The inverted-green channel of fundus images were preprocessed by equalizing illumination and contrast enhancement followed by smoothing. Candidates were then extracted by profile analysis and region growing. Intensity and shape features were extracted from MA candidates region. Four supervised classifier were selected; K-Nearest Neighbor (KNN), Naïve Bayes (NB) and Adaboost.

3. IMAGE PROCESSING

3.1 DATABASE [6]

- e-ophtha is a database of color fundus images especially designed for scientific research in Diabetic Retinopathy (DR).
- It has been generated from the OPHDIAT© Tele-medical network for DR screening, in the framework of the ANR-TECSAN-TELEOPHTA project funded by the French Research Agency (ANR).
- e-ophtha is made of two sub databases named **e-ophtha-MA (MicroAneurysms)**, and e-ophtha-EX (EXudates). I have used e-ophtha-MA database for this project.
- The database is a zipped file that contains folders. Each folder corresponds to a patient visit.
- It includes one or more color fundus images (.jpeg files) and binary masks made of lesions (.png files). Images of healthy patients with no lesion are also provided in the database.
- It contains 148 images with 1306 microaneurysms and 233 images with no lesion.
- Due to high contrast, green channels of color fundus images are considered.
- The images of healthy subjects and the ground truth images of patients are used for training purpose whereas the patient data is used for testing the model.
- Some of the patient database images are:

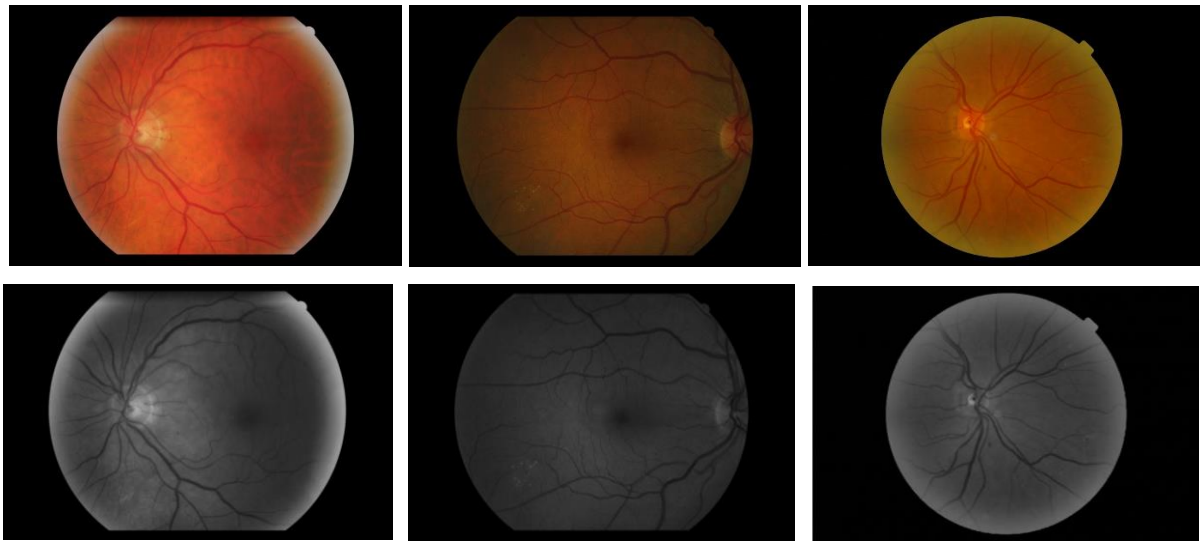

Figure 3.1: Color fundus Images and their green channel

3.2 BLOCK DIAGRAM

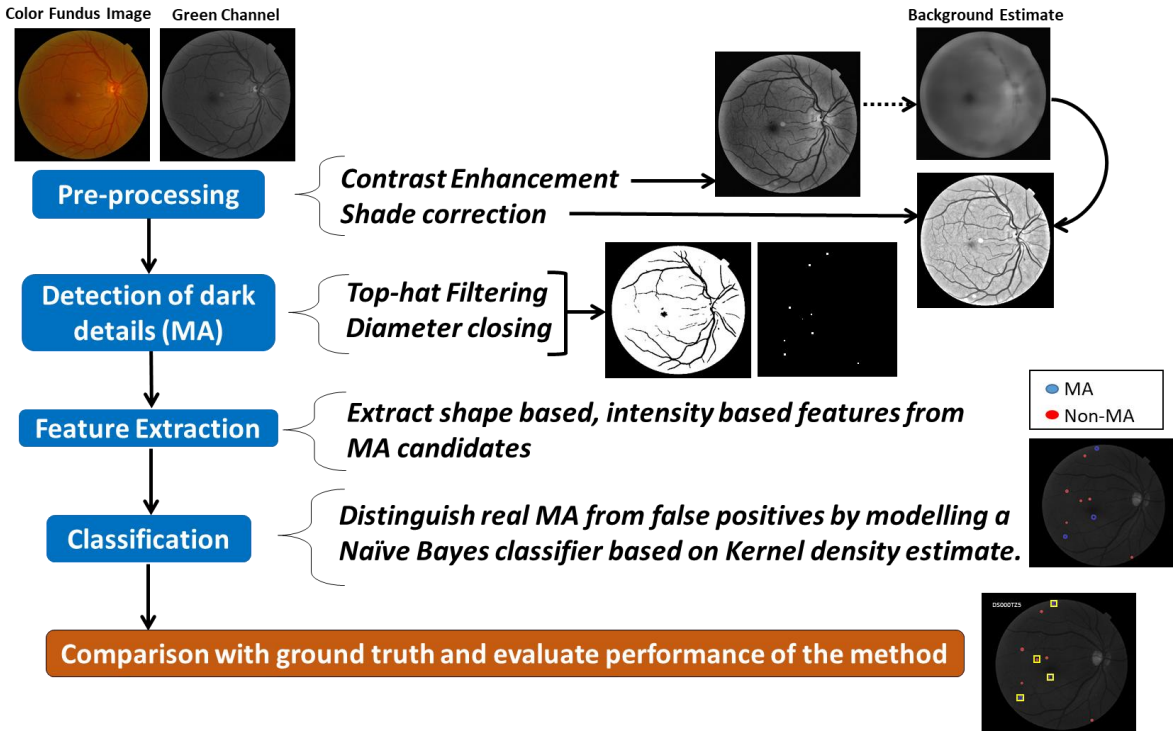

Figure 3.2: Block Diagram

3.3 PRE-PROCESSING

Detection of MAs is challenging due to the variation in MA size, low and varying contrast and variation in fundus image background. Color fundus images often suffer from non-uniform illumination, poor contrast and noise. The preprocessing step aims at attenuating these imperfections.

3.3.1 De-noising and smoothing

- The green channel of color fundus images are de-noised using median filter to remove salt and pepper noise that are main noises effects in retinal images.
- Output of Denoising:

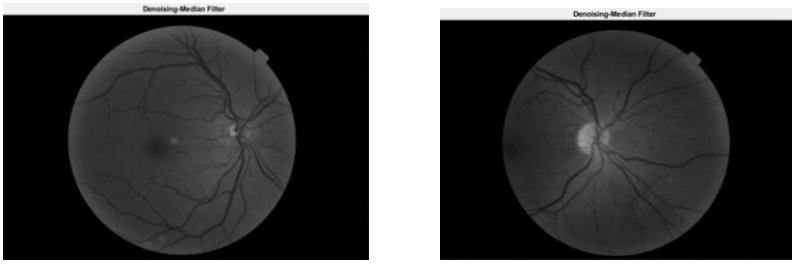

Figure 3.3.1: Denoising and Smoothing (Image 1 & Image 2)

3.3.2 Contrast Enhancement

- Contrast-limited Adaptive Histogram Equalization (CLAHE) technique is used.
- It enhances the contrast of images by transforming the values in the image.
- It operates on small data regions (tiles), rather than the entire image.
- Each tile's contrast is enhanced, so that the histogram of the output region approximately matches the specified histogram.
- The neighboring tiles are then combined using bilinear interpolation in order to eliminate artificially induced boundaries.
- Thus, enhancing the contrast makes dark details such as MA, relatively much darker.

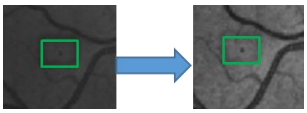

- Output of Contrast enhancement:

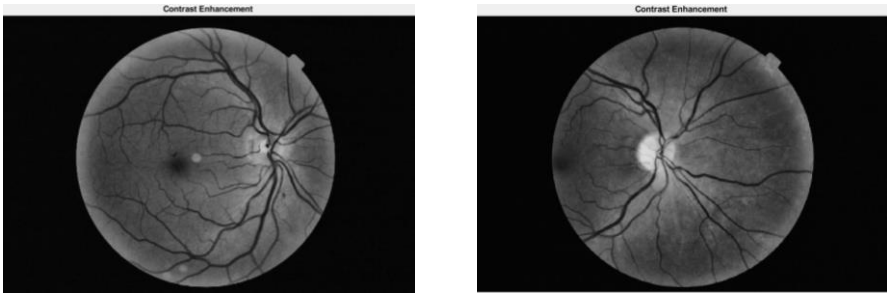

Figure 3.3.2: Contrast enhanced (Image 1 & Image 2)

3.3.3 Shade Correction

- Shade Correction helps to remove unwanted changes in intensity that occurred across the image due to the photographic process and to choroidal fluorescence.
- To do this, median filter with large window size such as [78 78] is applied to the images obtained from previous step.
- This gives the background illumination estimation used to correct shade variations.
- Since, the fundus images are stored in a lossy compressed form (.jpg), structures such as MAs are distorted.
- Also, due to the small size of MAs, it is important to reduce the effect of noise. Thus, it is necessary to consider image smoothing before performing MA detection and the shade corrected images are Gaussian filtered to attenuate the noise.
- Output images of shade corrected and Gaussian filtered images:

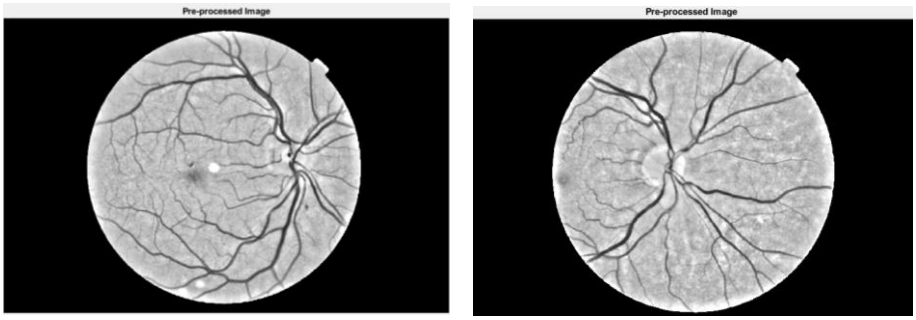

Figure 3.3.3: Shade Corrected (Image 1 & Image 2)

3.4 MICROANEURYSM CANDIDATE DETECTION

The objective of this step is to find initial set of 'MA candidates' where MAs are likely to exist. The goal is to reduce the number of detected objects which is not similar to MAs without losing any true MAs, as they cannot be retrieved later.

3.4.1 Top-hat Filtering

- A linear structuring element is used for performing morphological closing on the preprocessed image along a range of directions to extract blood vessels.

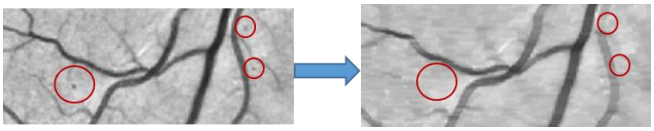

- The preprocessed image is then subtracted from the top-hat filtered image.

3.4.2 Diameter Closing

- Morphological closing with disk as structuring element is performed which fills the holes inside the circular dark details that are MA candidates and are converted into binary image. The connected components such as candidate regions are labeled.
- Output images of blood vessels (binary version) and MA candidates detection:

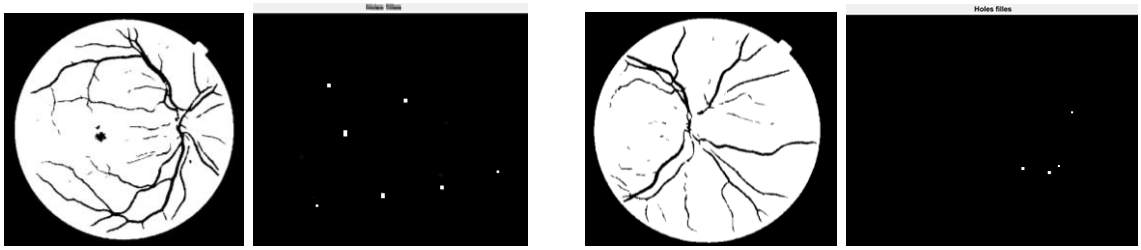

Figure 3.4.2: Blood vessels extracted and MA Candidates detected (Image 1 & Image 2)

4. FEATURE EXTRACTION AND CLASSIFICATION

4.1 FEATURE EXTRACTION FROM MA CANDIDATES

I have used 11 features in order to distinguish real MA from false positives (FP). Features are extracted from each candidate detected. These features are based on shape and intensity of the MA candidates. Energy and homogeneity were obtained using Gray Level Co-occurrence Matrix (GLCM).

4.1.1 Shape based features (computed on binary version)

i. **Area**: Actual number of pixels in the MA candidate region.

ii. P**erimeter**: It is the boundary that surrounds the area of candidate region.

iii. **Eccentricity**: Ratio of the distance between the foci of the ellipse and its major axis length. An ellipse whose eccentricity is 0 is actually a circle, while an ellipse whose eccentricity is 1 is a line segment.

iv. **Extent**: Ratio of pixels in the MA candidate region to pixels in the total bounding box computed as the Area divided by the area of the bounding box.

v. **Aspect Ratio**: Ratio of the length of major axis to minor axis of candidate region.

vi. **Orientation**: Angle between the x-axis and the major axis of the ellipse.

4.2 Intensity based features (computed on grayscale version)

i. **Max Intensity**: Value of the pixel with the greatest intensity in MA candidate region.

ii. **Mean Intensity**: Mean of all the intensity values in the MA candidate region.

iii. **Min Intensity**: Value of the pixel with the lowest intensity in MA candidate region.

iv. **Energy**: Reflects the uniformity of candidate's gray distribution and texture thickness. Energy=$\sum_{i,j} P(i,j)^2$

v. **Homogeneity**: Reflects the tightness of distribution of elements to the diagonal in GLCM. Homogeneity = $\frac{=\sum i,j P(i,j)}{(1+|i-j|)}$

	A	B	C	D	E	F	G	H	I	J	K	L
1	Label	Area	Perimeter	Eccentricity	Extent	Aspect Ratio	Orientation	MaxIntensity	MeanIntensity	MinIntensity	Energy	Homogeneity
2	falsePos(Non-MA)	6	5.905	0.63245553	0.666667	1.290994449	45	0.120639981	0.108494786	0.10148831	0.111111	0.551388889
3	falsePos(Non-MA)	4	3.556	0	1	1	0	0.115398366	0.11054003	0.105587638	0.222222	0.833333333
4	falsePos(Non-MA)	6	5.516	0.74535599	1	1.5	90	0.110955328	0.10497979	0.100610261	0.135802	0.666666667
5	falsePos(Non-MA)	3	3.093	0.73029674	0.75	1.463850109	-45	0.106706835	0.103908859	0.10093542	0.166667	0.588888889
6	falsePos(Non-MA)	4	3.556	0	1	1	0	0.104984034	0.103350354	0.101836237	0.277778	0.638888889
7	falsePos(Non-MA)	2	1.96	0.8660254	1	2	0	0.102560773	0.101460997	0.100361221	0.333333	0.527777778
8	falsePos(Non-MA)	2	1.96	0.8660254	1	2	90	0.107526236	0.106413633	0.10530103	0.25	0.583333333
9	falsePos(Non-MA)	5	4.962	0.76509206	0.833333	1.552985739	-71.5650512	0.116821573	0.112184829	0.100955276	0.135802	0.601851852
10	falsePos(Non-MA)	6	5.905	0.63245553	0.666667	1.290994449	45	0.117562238	0.107044589	0.101699587	0.111111	0.421626984
11	falsePos(Non-MA)	1	0	0	1	1	0	0.10231977	0.10231977	0.10231977	0.5	1
12	falsePos(Non-MA)	4	3.556	0	1	1	0	0.111356066	0.11036685	0.109533472	0.222222	0.347222222
13	falsePos(Non-MA)	1	0	0	1	1	0	0.100898228	0.100898228	0.100898228	0.5	1
14	falsePos(Non-MA)	1	0	0	1	1	0	0.102273932	0.102273932	0.102273932	0.5	0.291666667
15	falsePos(Non-MA)	1	0	0	1	1	0	0.101604494	0.101604494	0.101604494	0.5	0.291666667
16	falsePos(Non-MA)	6	5.516	0.74535599	1	1.5	90	0.114110591	0.10941894	0.103720479	0.135802	0.444444444
17	falsePos(Non-MA)	5	4.962	0.76509206	0.833333	1.552985739	-18.4349488	0.119554815	0.111881117	0.102652323	0.15625	0.541666667
18	falsePos(Non-MA)	4	3.556	0	1	1	0	0.102165366	0.100967179	0.100020072	0.5	0.888888889
19	falsePos(Non-MA)	1	0	0	1	1	0	0.100416772	0.100416772	0.100416772	0.5	0.666666667
20	falsePos(Non-MA)	1	0	0	1	1	0	0.102883243	0.102883243	0.102883243	0.5	0.75
21	falsePos(Non-MA)	8	6.831	0.5809475	0.888889	1.228590234	-45	0.13049264	0.116562967	0.106660958	0.097222	0.495833333
22	falsePos(Non-MA)	2	1.96	0.8660254	1	2	0	0.105897768	0.104125969	0.10235417	0.333333	0.611111111
23	falsePos(Non-MA)	3	3.093	0.73029674	0.75	1.463850109	-45	0.110763005	0.106934274	0.104166028	0.166667	0.597222222

[- 24 to 5274 -]

5275	truePos(MA)	16	12.364	0.51582595	0.64	1.167278744	-26.9678069	0.233039532	0.174626702	0.100215052	0.04	0.396984127
5276	truePos(MA)	35	25.745	0.23565183	0.555556	1.028978563	24.11985015	0.234665794	0.175899888	0.065799018	0.019184	0.472930839
5277	truePos(MA)	10	8.998	0.51314996	0.625	1.165095193	-45	0.229375222	0.197316842	0.155861129	0.055	0.286369048
5278	truePos(MA)	21	16.383	0.40636867	0.6	1.094440113	-0.36726052	0.200819498	0.145024073	0.054474572	0.0325	0.429613095
5279	truePos(MA)	14	10.106	0.6520712	0.875	1.318986743	-45	0.194715658	0.141937185	0.046256678	0.06	0.482142857
5280	truePos(MA)	7	6.368	0.35309393	0.777778	1.068846684	90	0.089896673	0.052213262	0.018914042	0.097222	0.385416667
5281	truePos(MA)	7	6.368	0.35309393	0.777778	1.068846684	90	0.095050423	0.05438656	0.020697612	0.125	0.477777778
5282	truePos(MA)	6	6.186	0.83333333	0.666667	1.809068067	53.13010235	0.134487163	0.103355992	0.069794204	0.083333	0.28505291
5283	truePos(MA)	16	12.364	0.88023643	0.64	2.107324447	45	0.231900275	0.198007626	0.157066252	0.035556	0.305661376
5284	truePos(MA)	7	6.368	0.35309393	0.777778	1.068846684	90	0.138104241	0.094521464	0.037514439	0.111111	0.266170635
5285	truePos(MA)	14	12.091	0.53833148	0.56	1.186615192	56.88617441	0.291545721	0.230436812	0.130167204	0.037778	0.39281746
5286	truePos(MA)	17	13.29	0.73461582	0.708333	1.473875623	3.446211561	0.181220265	0.13061322	0.062255004	0.040816	0.417346939
5287	truePos(MA)	56	35.041	0.56413611	0.509091	1.211120301	28.68581347	0.337003781	0.197491489	0.025430307	0.020417	0.443015873
5288	truePos(MA)	8	8.626	0.19364917	0.5	1.019294383	-45	0.127046933	0.100402356	0.066843622	0.055	0.370833333
5289	truePos(MA)	10	10.313	0.52718987	0.625	1.176820148	-30.9637565	0.197588624	0.160238231	0.101685568	0.05	0.468809524
5290	truePos(MA)	15	16.218	0.75681024	0.5	1.529906655	44.31803623	0.223407929	0.172941406	0.116182444	0.035494	0.400925926
5291	truePos(MA)	34	24.455	0.53666429	0.607143	1.185120783	-3.61330225	0.272544682	0.185823254	0.075845265	0.026959	0.427910053
5292	truePos(MA)	91	31.84	0.49004375	0.752066	1.147186508	90	0.138187842	0.037313627	0.001644501	0.016529	0.411664262
5293	truePos(MA)	6	6.277	0.45643546	0.666667	1.123902974	26.56505118	0.151017967	0.116009239	0.080725535	0.083333	0.246626984
5294	truePos(MA)	20	13.472	0.68386302	0.833333	1.370594457	-5.40471517	0.250295012	0.181608875	0.123963426	0.048469	0.519047619
5295	truePos(MA)	16	12.736	0.73516849	0.666667	1.475177717	21.30994143	0.261060095	0.208967412	0.154968763	0.038265	0.369430272
5296	truePos(MA)	8	6.831	0.5809475	0.888889	1.228590234	45	0.145107078	0.08118662	0.036329394	0.083333	0.336855159
5297	truePos(MA)	13	16.747	0.7281439	0.541667	1.458950328	-36.7285083	0.189533953	0.137299831	0.045731566	0.045918	0.422363946

Figure 3.5: Feature Vector Trained Dataset

- 50 healthy patient's images and 60 diseased patient's ground truth images are used for training and their feature values are stored in an excel sheet.
- Feature values such as area, perimeter, eccentricity, ratio of major and minor axis length i.e. aspect ratio, orientation, maximum, minimum, and mean intensity values, energy and homogeneity are displayed in the excel sheet.
- MA candidates detected in healthy patient's data are treated as False Positives (Non-MA) and those detected from ground truth images of diseased patients are treated as True Positives (MA).

4.2 CLASSIFICATION OF DETECTED MA CANDIDATES

Here, the classification is pixel-based as each MA candidate pixel is classified as MAs or non-MAs independently from its neighbor.

Features of each candidate training data are extracted and are fed with correct class labels (MA: 1, non-MA: 0) as input to the classifier.

After training, the class of the unit with the maximum value is determined to be the corresponding class to which an unknown sample (MA candidate) belongs.

4.2.1 Naive Bayes classification model using estimated kernel densities

- A Naive Bayes classifier is a conditional probabilistic classifier based on applying Bayes' theorem with strong (naive) independence assumptions. It assumes that the features are conditionally independent given the class; $p(x \mid C_k) = \pi_i\, p(x_i \mid C_k)$
- A kernel is a weighting function used in non-parametric estimation techniques. They are used in kernel density estimation to estimate random variable's density functions. Non-parametric estimators have no fixed structure and depend upon all the data points to reach an estimate.
- A kernel distribution is defined by a smoothing function (Gaussian) and a bandwidth value (h) which control the smoothness of the resulting density curve.
- Choosing 'h' is crucial in density estimation (DE);

Large h (broad kernels) → low variance and high bias (over-smooth the DE and mask the structure of the data)

Small h (narrow kernels) → high variance and low bias (yield a DE that is spiky and very hard to interpret)

The bandwidth h is estimated for each combination of predictor and class by using a value that is optimal for a Gaussian distribution. Use large h in regions with low sample density in order to obtain a smooth estimation, and use low h in high density regions.

1. *Training step*: Using the training data, the method estimates the parameters of a probability distribution, assuming predictors (feature vectors) are conditionally independent given the class.
2. *Prediction step*: For a given MA candidate to be classified, represented by a vector representing the features extracted (independent predictor variables), it calculates the posterior probabilities $p(C_k \mid x_1, \ldots..x_n)$ for each of (k=2) possible outcomes or classes. The class with the maximum posterior probability will be chosen.

Using Bayes' theorem, the conditional probability can be decomposed as;

$$p(Ck|x) = \frac{p(Ck)\, p(x|Ck)}{p(x)}$$

The method then classifies the test data according the largest posterior probability. The class label assigned to the MA candidate is given by;

$$C_k = argmax_{Ck}\, p\,(C_k \mid x)$$

where $p(x| C_k)$ is the likelihood of feature vector x given class C_k, and $p(C_k)$ is the priori probability of class C_k.

Output images of identifying labels of MA candidates:

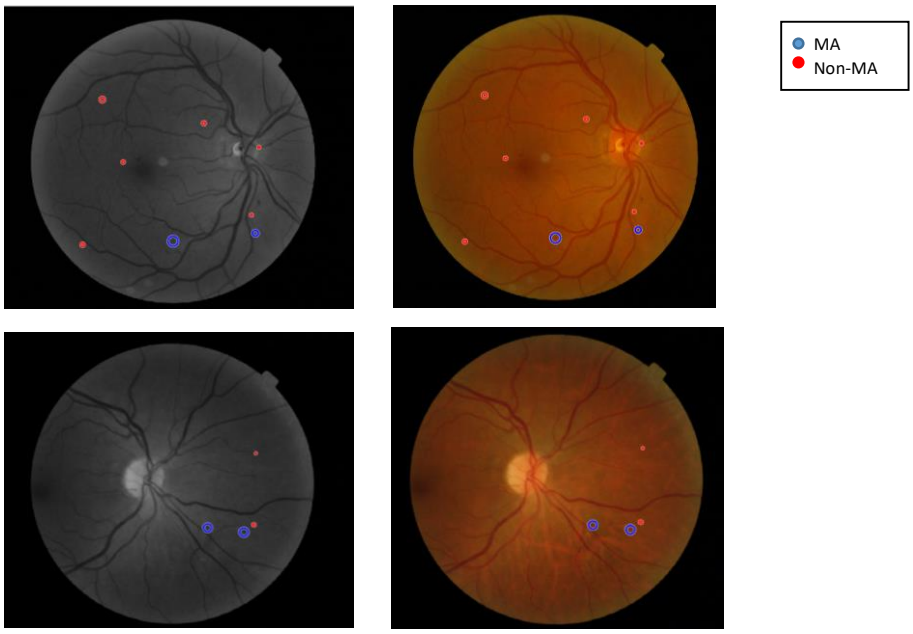

Figure 3.6: MA candidates classified as MA (blue circles) and non-MA (red circles)

4.3. ALGORITHM

In this section, the steps performed and the algorithms used in each of the module of the project have been discussed.

a) Steps for pre-processing:

Step 1: Median filtering is perform to remove salt and pepper noise, if any.

Step 2: Green channel is extracted from the color fundus image

Step 3: Local histogram equalization is performed.

Step 4: Background Image is obtained and shade correction is performed.

Step 5: Gaussian smoothing to attenuate noise.

b) Steps for MA candidate's detection:

Step 1: Linear Structuring Element is created acting along many possible directions and morphological operations is done to detect fine vessels and MA structures.

Step 2: Top-hat filtering is done to remove vessels.

Step 3: Morphological closing with disk structuring element fills holes in MA regions.

Step 4: The image is then binarized and the connected components are labeled.

c) Steps for training the data:

Step 1: Images from the training database are selected.

Step 2: Shape based and Intensity based features are extracted.

Step 3: The feature values are then stored in an excel sheet with the labels.

d) Steps for building model and perform classification:

Step 1: Excel Spreadsheet is read which was created in Step 3 of c).

Step 2: The data is spitted into training (70%) and testing data (30%) by and a Naive Bayes classifier model with kernel distributions is created by fitting training data.

Step 3: The testing data is called and its label is predicted.

Step 4: If the prediction is true Positive, the region is encircled with blue color else it is encircled with red color.

5. RESULTS AND DISCUSSION

True Positive (TP) → indicates that MA is correctly predicted.

True Negative (TN) → indicates that non-MA is correctly predicted.

False Positive (FP) → indicates that non-MA is erroneously predicted as MA

False Negative (FN) → indicates that MA is erroneously predicted as non-MA.

Performance of the method and the trained model evaluated by confusion matrix

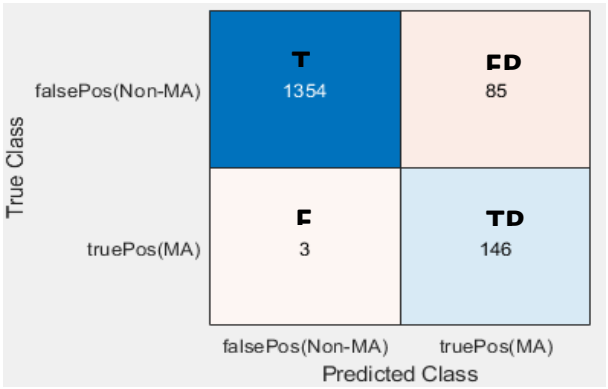

Figure 5.1: Confusion matrix

Following metrics are used to evaluate the trained model;

- **Sensitivity (or Recall)** is the percentage of true positives. It is the proportion of MA candidates who are correctly identified as MAs among all those who actually are the MA.

$$\text{Sensitivity} = \frac{\text{TP}}{\text{TP+FN}} = 0.9798 = 97.98\%$$

- **Specificity** is the percentage of true negatives. It is the proportion of MA candidates that are correctly identified as non-MA among all those who actually are non-MAs.

$$\text{Specificity} = \frac{\text{TN}}{\text{TN+FP}} = 0.9409 = 94.09\%$$

- **Positive Predictive Value (PPV) (or Precision)** is the probability of true positive MAs classified among other positive test result i.e. correctly classified MA samples divided by the classified MAs.

$$\text{Positive predictive value (PPV)} = \frac{\text{TP}}{\text{TP+FP}} = 0.6302 = 63.02\%$$

- **Negative Predictive Value (NPV)** is the probability of true non-MAs classified among other non-MA test result i.e. correctly classified non-MA samples divided by the classified non-MAs.

$$\text{Negative predictive value (NPV)} = \frac{TN}{TN+FN} = 0.9977 = 99.77\ \%$$

- **Accuracy** is the proportion of the total number of predictions (MA or non-MA) that were correct.

$$\text{Accuracy} = \frac{TP+TN}{TP+TN+FP+FN} = 0.9445 = 94.45\ \%$$

Comparison of model results with ground truth;

For comparing the MA candidates classified by the model with the ground truth provided along with the database, I have used sensitivity, specificity, PPV, NPV and accuracy as merit of figure to evaluate the performance of the system.

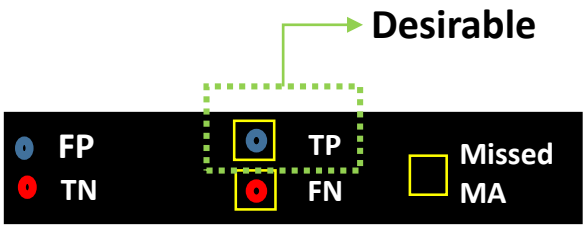

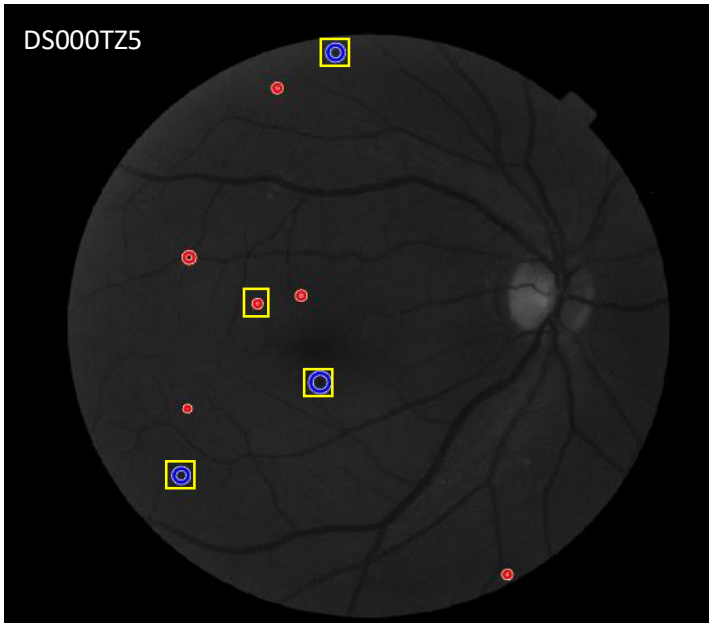

Figure 5.2: Output image 1

$$\text{Sensitivity} = \frac{TP}{TP+FN} = \frac{3}{3+1} = 75\%$$

$$\text{Specificity} = \frac{TN}{TN+FP} = \frac{5}{5+0} = 100\%$$

$$\text{PPV} = \frac{TP}{TP+FP} = \frac{3}{3+0} = 1$$

$$\text{NPV} = \frac{TN}{TN+FN} = \frac{5}{5+1} = 0.83$$

$$\text{Accuracy} = \frac{TP+TN}{TP+TN+FP+FN} = \frac{8}{9} = 88.89\%$$

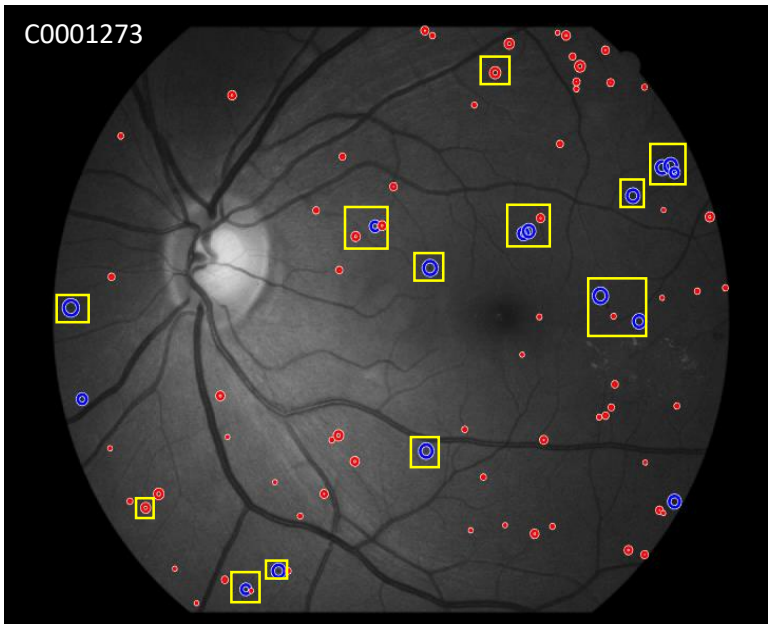

Figure 5.3: Output image 2

$$\text{Sensitivity} = \frac{TP}{TP+FN} = \frac{14}{14+7} = 66.67\%$$

$$\text{Specificity} = \frac{TN}{TN+FP} = \frac{58}{58+2} = 96.67\%$$

$$\text{PPV} = \frac{TP}{TP+FP} = \frac{14}{14+2} = 0.87$$

$$\text{NPV} = \frac{TN}{TN+FN} = \frac{58}{58+7} = 0.89$$

$$\text{Accuracy} = \frac{TP+TN}{TP+TN+FP+FN} = \frac{8}{9} = 88.89\%$$

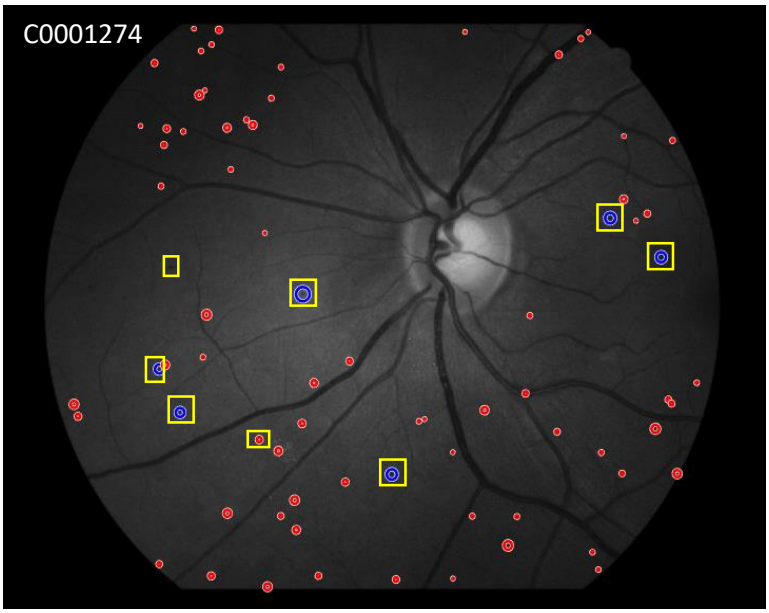

Figure 5.4: Output image 3

$$\text{Sensitivity} = \frac{TP}{TP+FN} = \frac{6}{6+1} = 85.71\%$$

$$\text{Specificity} = \frac{TN}{TN+FP} = \frac{68}{68} = 100\%$$

$$\text{PPV} = \frac{TP}{TP+FP} = \frac{6}{6} = 1$$

$$\text{NPV} = \frac{TN}{TN+FN} = \frac{68}{68+1} = 0.985$$

$$\text{Accuracy} = \frac{TP+TN}{TP+TN+FP+FN} = \frac{74}{75} = 98.6\%$$

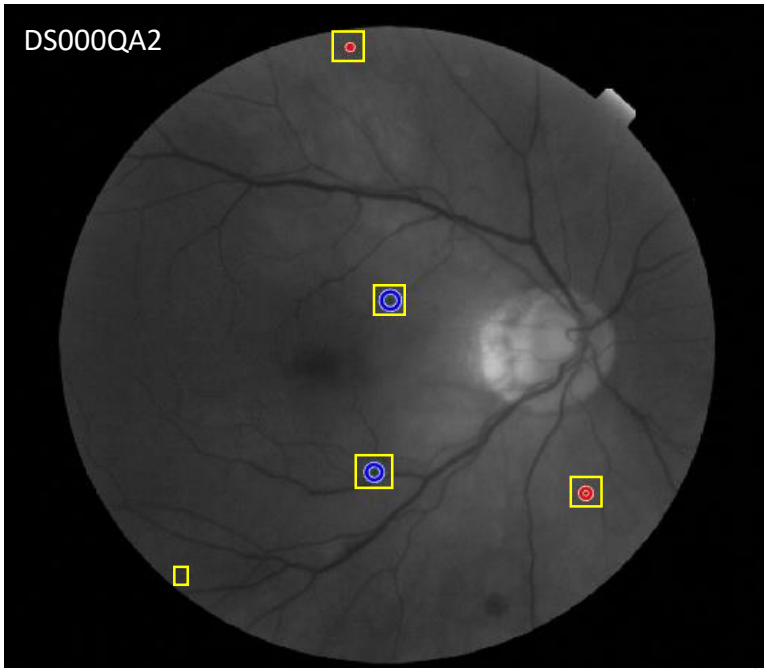

$$\text{Sensitivity} = \frac{TP}{TP+FN} = \frac{2}{2+2} = 50\%$$

$$\text{Specificity} = \frac{TN}{TN+FP} = \frac{TN}{TN+0} = 100\%$$

$$PPV = \frac{TP}{TP+FP} = \frac{2}{2+0} = 1$$

$$NPV = \frac{TN}{TN+FN} = \frac{0}{0+2} = 0$$

$$\text{Accuracy} = \frac{TP+TN}{TP+TN+FP+FN} = \frac{2}{4} = 50\%$$

Figure 5.5: Output image 4

From the overall observations, it could be concluded that the algorithm was quite effective to detect all possible MA candidates with very low percentage of missing few of them.

Furthermore, it could be observed that sensitivity, which is percentage of true positives, was found to be as high as nearly 85% and as low as nearly 50%. This shows that our classification model may sometime erroneously classify actual MA as non-MA, which is not desirable. However, this could be improved with better selection of features from MA candidates and model the classifier using other approach (such as ensemble classifier, neural network).

The model performs well in classifying non-MA from the detected MA candidates. This could be justified from the specificity value, which is percentage of true negatives, goes to maximum of 100%.

5. LIMITATIONS AND FUTURE SCOPE

5.1 Limitations

1) One of the main limitations of this study could be the interference of image noises, hemorrhage or laser burns on MA detection. Sometime, it's difficult to distinguish MA and similar structures present in the image, using the approach mentioned.

2) Insufficient processing to removes vessel crossings and blood vessels in the retina data may result in false positive cases.

3) The parameters for image processing cannot be generalized for any given dataset due to variation in image properties belonging to different datasets.

5.2 Future scope of the project

1) For the limitations mentioned above, it's important to improve de-noising step.

2) The accuracy of the MA detection algorithm can be improved by performing different segmentation techniques (such as circular Hough transform) to extract blood vessels (especially, thin vessel fragments) and other non-MA features.

3) To generalize the method, more databases should be considered covering all types of variations which can be possible in retinal images, in case of DR, so that there is no ideal conditions assumed.

4) Also, the improved method can be combined with an algorithm for the detection of hemorrhages and an algorithm for the detection of exudates to make it very helpful to the ophthalmologists in detecting MA and become more likable for clinical uses.

REFERENCES

[1] Automatic detection of microaneurysms in color fundus images by Thomas Walter, Pascale Massin, Ali Erginay, Richard Ordonez, Clotilde Jeulin, Jean-Claude Klein, https://www.sciencedirect.com/science/article/abs/pii/S1361841507000461

[2] Automatic Detection of Microaneurysms in Color Fundus Images of the Human Retina by Means of the Bounding Box Closing Thomas Walter and Jean-Claude Klein, https://link.springer.com/chapter/10.1007%2F3-540-36104-9_23

[3] Automatic Recognition of Microaneurysms in Diabetic Retinopathy by Lay et.al, 1983 (FA), https://www.researchgate.net/publication/267694958_Automatic_Recognition_of_Microaneurysms_in_Diabetic_Retinopathy

[4] Automated detection and quantification of microaneurysms in fluorescein angiograms by Spencer, 1991 et al. (FA), https://link.springer.com/article/10.1007/BF00166760

[5] mipav.net/MIPAV%20Papers/2018-1-22/吴波1-s2.0-S0895611116300787-main.pdf

[6] http://www.adcis.net/en/third-party/e-ophtha/, Decencière E, et al. TeleOphta: Machine learning and image processing methods for teleophthalmology. IRBM (2013), http://dx.doi.org/10.1016/j.irbm.2013.01.010